Int j simul model 15 (2016) 4, 754-765
ISSN 1726-4529 Original scientific paper

MODELLING THE DYNAMICS AND SECONDARY DEFORMATION BEHAVIOUR OF THE STRIP WITH LOCAL WAVES IN COILING PROCESS

Sun, W. Q.[*]; Guan, J. L.[**]; Shao, J.[*] & He, A. R.[*]
[*] Engineering Research Institute, University of Science and Technology Beijing, Beijing 100083, China
[**] Beijing Zongheng Electro-Mechanical Technology Development Co., Beijing 101407, China
E-Mail: wqsun18@163.com, guanjianlong@aliyun.com, ustbshao@163.com, harui@ustb.edu.cn

Abstract
With the introduction of 3D elastic-plastic deformation, and strip plastic flow factor concept, to analysis of the influence of strip local high points on the ridge-buckle behaviour in coiling process, an elastic-plastic coiling stress and ridge-buckle value model that can be used for online calculation was established. According to comparison and analysis of the influencing factors, uneven distribution of radial and circumferential stress caused by local waves is an important cause of strip ridge-buckle, and the ridge-buckle value increases with increases of local wave size, coil diameter and coiling tension, and significantly with decreases in the strip thickness. The influence of waves with different locations on the ridge-buckle value was analysed. Based on comparison of analysis results obtained by an elastic ridge-buckle value model and ANSYS FEM (finite element method), the accuracy and feasibility of this model have been proved, which will provide theoretical and model support for subsequent reduction of the ridge-buckle defects brought by local waves.
(Received, processed and accepted by the Chinese Representative Office.)

Key Words: Local Waves, Elastic-Plastic Deformation, Plastic Flow Factor, Ridge-Buckle, ANSYS FEM

1. INTRODUCTION

A ‘ridge buckle’ defect refers to a ‘bulge’ that appears on a coil surface. This is due to the accumulation, by layer, of local features, including a local thickness high point and local waves shapes, as well as an uneven distribution of local residual stress and other features acting during the coiling process. Ridge buckle, as shown in Fig. 1, is particularly prominent on thin strip metal and greatly affects the quality of high precision cold rolled metal strip. If there are a large number of ridge buckles, an additional small waves shape will appear after the coil has been uncoiled, as shown in Fig. 2. This has a serious impact on product performance and appearance [1]. Due to the complex mechanism of the “ridge-buckle” phenomenon, it has not been explained in a rational and correct way and for many years has been a technical problem that seriously troubles production, and needs to be solved urgently [2]. At present, researches on ridge buckles as well as methods for calculating coiling stress and ridge-buckle value are all based on the theory of elasticity. Melfo, Zhu and other scholars have studied the microstructural and temperature features of hot strips that may lead to ridge-buckle defects in thin-rolled steel strip [3-5]; Bai supposes that waves are present before coiling and calculates the amount of ridge buckles after the coiling of local waves [6]; Ovesy et al. and Lorenzini et al. researched the buckling and post-buckling behaviour of moderately thick plates using an exact finite strip [7, 8]. In the actual coiling process, the strip exhibits local plastic deformation and there is metal plastic flow if the degree of ridge buckle achieves a certain amount [9]. Therefore, the theory of elasticity is no longer applicable to the calculation of coiling stress and ridge-buckle value of ridge-buckle coil. In this paper, with reference to some ideas on how to deal with 3D elastic-plastic deformation and introduction of strip plastic flow factors, an elastic-plastic coiling stress and ridge-buckle value model was

established, that can be used for online calculation and also provides a theoretical basis for online control over ridge buckles.

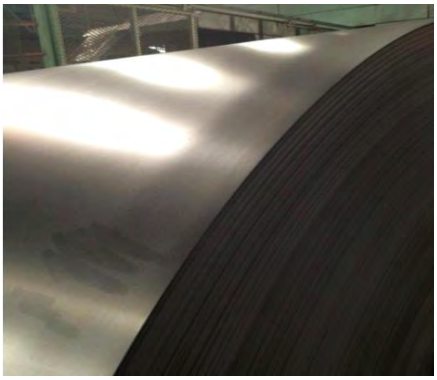

Figure 1: Physical map of a strip with ridge buckle.

Figure 2: Physical map of ridge buckle after uncoiling of a ridge buckle strip.

2. COILING STRESS AND RIDGE-BUCKLE VALUE ANALYTICAL MODEL

2.1 Geometric equation and equilibrium differential equation of coil

The geometric equation of strip coiling can be expressed as [8]:

$$\begin{cases} \varepsilon_r = \dfrac{\partial u}{\partial r}, \quad \varepsilon_\theta = \dfrac{u}{r} \\ \varepsilon_z = \dfrac{\partial w}{\partial z}, \quad \gamma_{zr} = \dfrac{\partial u}{\partial z} + \dfrac{\partial w}{\partial r} \end{cases} \tag{1}$$

where: u represents displacement along Axis r and w represents displacement of z axially.

The force analysis of steel coil is shown in Fig. 3, where the steel coil can be regarded as an axisymmetric anisotropic body, that is, deformation and stress of the strip are irrelevant to the polar angle. Therefore, the equilibrium differential equation of the unit under the column coordinate can be expressed as [10, 11]:

$$\begin{cases} \dfrac{\partial \sigma_r}{\partial r} + \dfrac{\partial \tau_{zr}}{\partial z} + \dfrac{\sigma_r - \sigma_i}{r} = 0 \\ \dfrac{\partial \sigma_z}{\partial z} + \dfrac{\partial \tau_{zr}}{\partial r} + \dfrac{\tau_{zr}}{r} + f_z = 0 \end{cases} \tag{2}$$

where: σ_r, σ_i, σ_z and τ_{zr} represent radial stress, circumferential stress, axial stress and shear stress of a steel coil unit, respectively, and f_z represents axial frictional force.

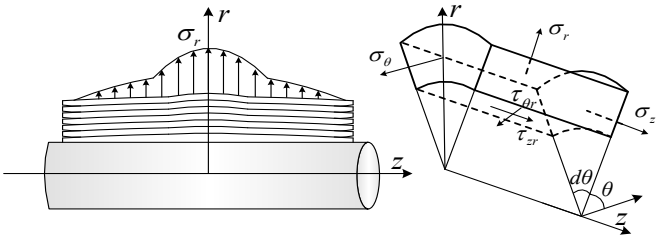

Figure 3: Analysis of the steel coil stress.

2.2 Physical equation of steel coil

As both stress tensor and tension tensor in the elastic-plastic physical equation can be decomposed into spherical tensor and deviator tensor, where volumetric deformation is proportional to spherical tensor of stress σ_m and shape distortion is related to stress deviator tensor, the strip's physical equation can be expressed as:

$$\varepsilon_{ij} = \varepsilon_{ii} + e_{ij} = \frac{1-2v}{E}\sigma_m \delta_{ij} + \lambda S_{ij} \tag{3}$$

where, ε_{ii} represents spherical tensor of tension, σ_m represents spherical tensor of stress, δ_{ij} represents spherical tensor of unit, e_{ij} represents tension deviator tensor, λ represents proportion coefficient between tension tensor and stress tensor.

For elastic deformation, λ=1/2 G; for elastic-plastic deformation, the proportional coefficient λ is related to position and load level, where $\lambda=3\varepsilon_i / 2\sigma_i$; ε_i and σ_i are tension intensity and stress intensity, respectively.

The elastic-plastic properties of the strip are determined by Mises yield conditions:

$$(\sigma_r - \sigma_i)^2 + (\sigma_i - \sigma_z)^2 + (\sigma_z - \sigma_r)^2 + 6\tau_{zr}^{\ 2} = 2\sigma_s^{\ 2} \tag{4}$$

where σ_s represents yield strength of the strip.

In the coiling process, the coiling tension is $\sigma_0(z)$ and circumferential compressing deformation $\varepsilon_\theta(z)$ occurs to the inner strip due to pressure from the outer strip, thus the resulting disappearance of strip tension can be expressed as (5):

$$\sigma_\theta(\mathrm{z}) = \sigma_0(\mathrm{z}) - \sigma_i(\mathrm{z}) \tag{5}$$

where, $\sigma_0(z)$ is axial distribution of strip coiling tension, $\sigma_i(z)$ is actual tension distribution of the strip Ring i among n rings that have been coiled.

2.3 Introduction of strip plastic flow factor

In the process of strip coiling, the plastic flow in strips is extremely limited in most regions except some local high points, so the deformation of strips can be largely regarded as in plane [12]. However, due to accumulation and superposition of local high points, radial and axial stress is distributed unevenly and forms a metal plastic flow state around local high points. Therefore, there is great difference between the centre and edge of the ridge buckle in transverse flow and the ratio of the axial tension deviator tensor e_z to the circumferential tension deviator tensor e_θ is not a constant. In order to describe the plastic flow state, an expression of the plastic flow factor is introduced to this paper and the strip plastic flow factor is defined as:

$$G = G(r, \theta, z) = e_z / e_\theta \tag{6}$$

According to the principle of volume invariably:

$$e_r + e_\theta + e_z = 0 \tag{7}$$

The relationship between tension and stress deviator tensors is:

$$\frac{e_r}{2\sigma_r - \sigma_\theta - \sigma_z} = \frac{e_\theta}{2\sigma_\theta - \sigma_r - \sigma_z} = \frac{e_z}{2\sigma_z - \sigma_r - \sigma_\theta} = \lambda \tag{8}$$

With Eqs. (6) and (7) substituted to (8), the relationship between axial, circumferential and radial stress deviator tensors can be shown as:

$$(2G+1)\sigma_\theta+(1-G)\sigma_r=(2+G)\sigma_z \tag{9}$$

With Eq. (9) substituted to the elastic-plastic physical equation, the strip plastic flow conditions can be reasonably introduced to differential calculations. Solving linear equations by the Cramer rule, the relationship between stress and tension of all coil units can be obtained, where M is the coefficient of the linear equation group:

$$\begin{cases}\sigma_r=M_1\varepsilon_r+M_2\varepsilon_\theta+M_2\varepsilon_z\\ \sigma_i(\mathrm{z})=-M_2\varepsilon_r-M_1\varepsilon_\theta-M_2\varepsilon_z-M_3\sigma_0\\ \sigma_z=M_2\varepsilon_r+M_2\varepsilon_\theta+M_1\varepsilon_z\\ \tau_{zr}=M_4\gamma_{zr}\end{cases} \tag{10}$$

2.4 Coil boundary conditions

1) Before the coil unwinds off the coiling drum, the coil inner surface's radial displacement u_0 is equal to that of the drum. δ_0 is flexibility coefficient of the drum:

$$\delta_0\sigma_r=u_0 \tag{11}$$

2) The shear stress on the inner surface of the coil is equal to the axial friction force between the coil and the drum:

$$\mu\sigma_r=M_4\left(\frac{\partial u}{\partial z}+\frac{\partial w}{\partial r}\right) \tag{12}$$

3) The outer surface of the coil is free, and both the radial stress component and the shear stress are zero:

$$\sigma_r=\tau_{zr}=0 \tag{13}$$

4) The strip circumferential stress on the outermost layer of the coil is equal to the coiling tension:

$$\int_{-z}^{z}\sigma_i(\mathrm{z})h(\mathrm{z})d_z=\int_{-z}^{z}\sigma_0h(\mathrm{z})d_z \tag{14}$$

5) The end face of the coil is free, and both the axial stress and the shear stress are zero:

$$\sigma_z=\tau_{zr}=0 \tag{15}$$

2.5 Axial distribution model of strip thickness and coil radius

Since there is a thickness difference or local high points on a strip along the width direction after cold rolling, the thickness distribution can be described by the convexity and local high points [13]:

$$h(z)=h(wz)+Y_r(z) \tag{16}$$

The axial thickness distribution of strip convexity is fitted by a profile gauge meter [14]:

$$h_{(wz)}=h_0\left\{\left[1-a\left(\frac{|z|}{b}\right)^c\right]+c_1\frac{|z|}{b}+c_2\frac{|z|^2}{b}\right\} \tag{17}$$

where: h_0 represents central strip thickness, b represents the half width of strip, a, c, c_1 and c_2 are strip convexity profile coefficients.

The axial thickness distribution of a local high point can be described by the quadratic function:

$$Y_r(z)=a_0+a_1X_r+a_2X_r^2 \tag{18}$$

where: x_r represents ridge-buckle width coefficient, a_0, a_1 and a_2 are profile coefficients of the local high point.

The axial distribution of coil radius can be calculated by the following formula [15]:

$$r_n(\mathrm{z}) = r_{\mathrm{n\text{-}1}}(\mathrm{z}) + h(\mathrm{z}) + l_n(\mathrm{z}) \tag{19}$$

where: $l_n(\mathrm{z})$ is the gap between strip layers, $l_n(\mathrm{z}) = l_0\, e^{-\zeta p}$; l_0 is the layer gap of the strip at the outermost layer, ζ is the radial compression coefficient and p the radial stress between layers.

The radial displacement u and the axial displacement w can be expressed as a function with r and z as variables. Let $u = f(r, z)$ and $w = \varphi(r, z)$. The displacement difference equations of all orders of the radial displacement u and the axial displacement w can be expressed as $f(r, z)$ and $\varphi(r, z)$. With Eqs. (1), (2), (16) and (19), as well as displacement difference equations substituted to Eq. (10), a differential equation expressed by two displacement functions can be obtained inside the coil, which covers equilibrium conditions, physical and geometrical equations:

$$\begin{cases} S_1 f_{i-1,j} - S_2 f_{i,j} + S_3 f_{i+1,j} + S_5\left(f_{i,j+1} + f_{i,j-1}\right) + S_6\left(\varphi_{i,j+1} - \varphi_{i,j-1}\right) \\ +S_4\left(\varphi_{i+1,j+1} + \varphi_{i-1,j-1} - \varphi_{i+1,j-1} - \varphi_{i-1,j+1}\right) - S_7 \dfrac{\sigma_0}{r} = 0 \\ L_1\left(f_{i+1,j+1} + f_{i-1,j-1} - f_{i+1,j-1} - f_{i-1,j+1}\right) + L_2\left(f_{i,j+1} - f_{i,j-1}\right) \\ +L_3\left(\varphi_{i,j+1} + \varphi_{i,j-1}\right) + L_4\varphi_{i+1,j} + L_5\varphi_{i-1,j} - L_6\varphi_{i,j} + f_z = 0 \end{cases} \tag{20}$$

where S and L are difference equation coefficients, f and φ are the radial and axial displacement functions of coil, respectively.

The basic dynamic programming is based on the optimization principle, and achieves the search of overall optimal solution. The precondition is the stages having no after-effect; namely, for the state of a certain given stage, the states of previous stages cannot directly affect its subsequent determination, which only depends on its current state [16].

In terms of hot rolling plant, the root cause for crown variance is the plastic deformation of the strip, while for single stand, the decisive factor of material deformation when applying load only relates to the stand itself rather than other stands. This means the "stages" of continuous mill plant has no after-effect. Based on this precondition, the dynamic programming-based profile allocation strategy can be established.

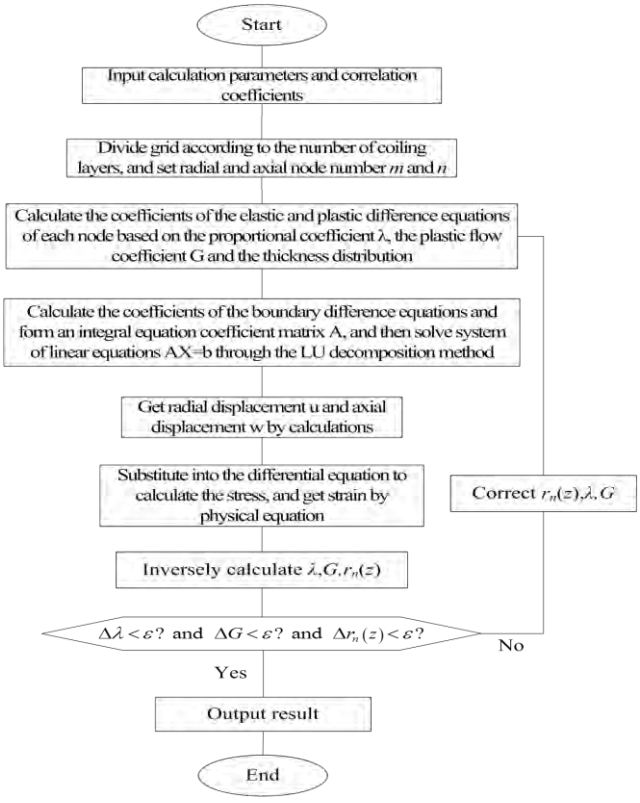

Figure 4: Calculation process of coiling strip stress model.

3. MODEL CALCULATION PROCESS

The solving procedure of the coiling stress and ridge-buckle value model is shown in Fig. 4. First divide the coil into a grid and set radial and axial node number m and n; make assumptions about the proportional coefficient λ and plastic flow factor G and determine the elastic-plastic difference equation coefficient according to the boundary conditions to form an integral equation coefficient matrix; then, solve a system of linear equations through the LU decomposition method to get the radial displacement u and the axial displacement w, and substitute them to the coiling stress difference equation and the physical equation to calculate stress and tension of each node; next, use the obtained stress and tension to inversely calculate the ratio coefficient λ of each node, plastic flow factor G and axial distribution of the coil diameter, and correct all coefficients to get the displacement, deformation and stress field of all layers of the strip.

4. ANALYSIS OF LOCAL-WAVES-CAUSED RIDGE-BUCKLE ANALYTICAL MODEL

4.1 Stress distribution of ridge-buckle coil

In view of the working condition parameters shown in Table I, the coil stress was simulated and the results are shown in Fig. 5.

The influence of initial flatness defects on the tension distribution and radial pressure distribution of layers gradually decreased with increasing coiling layers, where the initial shape had the greatest influence on tension distribution of the innermost layer of strip and the tension was the most uneven in the transverse distribution. The equivalent stress of the coil first decreased and then increased with the increase of coil diameter, for the inner strip of the coil, the strip had a slight transverse displacement in the width direction, thus producing an axial force that increased from strip edge to wave location, which is one of the main causes of the ridge-buckle appearance due to increased equivalent stress of the coil inner layer.

Table I: Calculated parameters.

Parameter size	**Value**	**Parameter size**	**Value**
Coil inner and outer diameter (mm)	300/900	Strip width (mm)	1000
Coiling tension (Mpa)	30	Strip thickness (mm)	0.5
Elasticity modulus (GPa)	205	Strip initial local waves (μm)	5 IU
Poisson's ratio (-)	0.3	Waves location (-)	Strip centre

For strip with local waves, a ridge buckle first appears in the innermost layer of the coil, which can be understood as: if the innermost strip of the coil has no ridge-buckle defects, another layer outside will suffer no ridge buckles. With the accumulated amount of ridge buckles inside the coil, the original flatness stress of the strip is lost and a continuous bulge will produce local additional axial and radial stress. Therefore, ridge buckles caused by local waves on the outer layer of the coil share the same mechanism as those caused to the strip due to local high points, both because the strip locally bulges, thus causing flexural buckling as a result of significant increases of strip local equivalent stress.

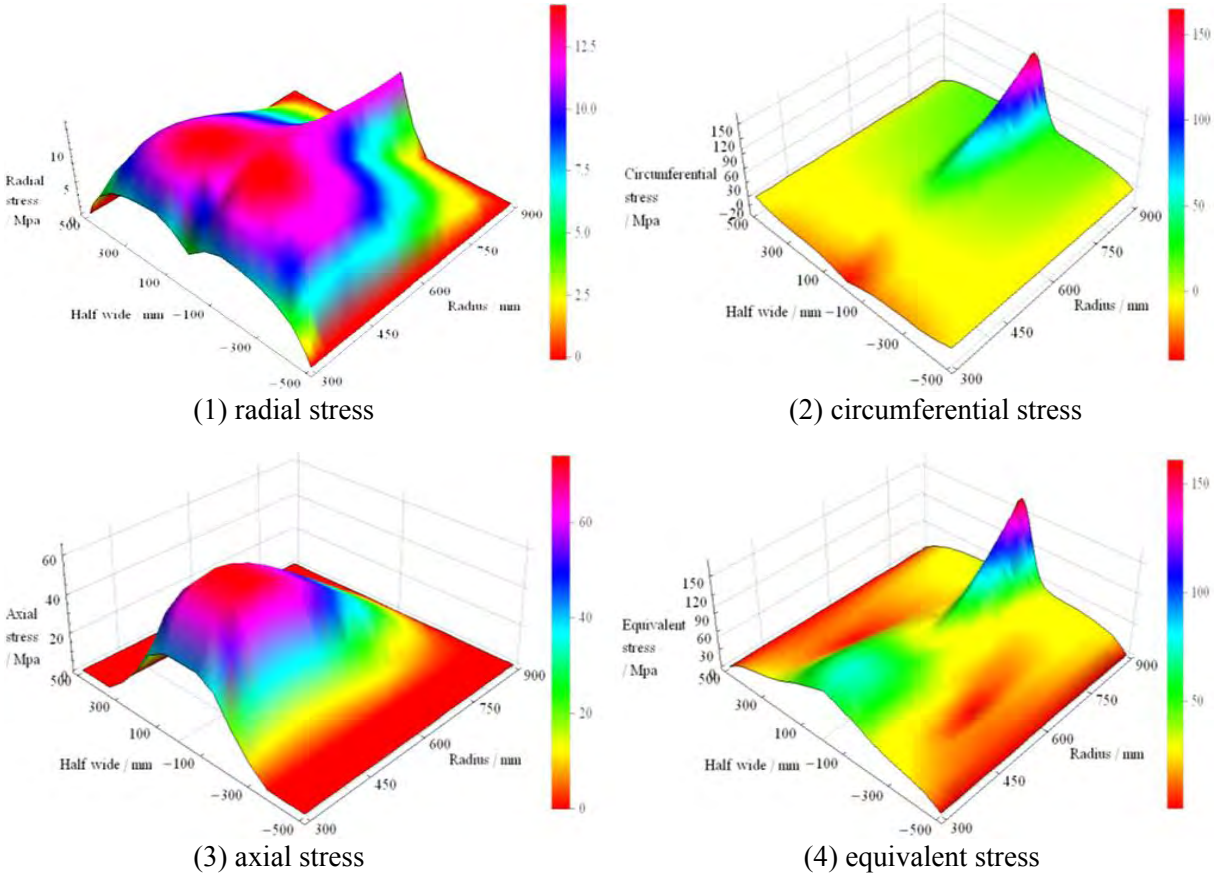

(1) radial stress (2) circumferential stress

(3) axial stress (4) equivalent stress

Figure 5: Stress distribution of the coil with central waves.

4.2 Relationship between coiling tension and strip ridge-buckle value

Calculations were performed for ridge-buckle values of strip pieces with a coiling tension of 20-50 Mpa, thickness of 0.5 mm, coil diameter of 900 mm, and local waves of 3-7 IU in the centre respectively and the results are shown in Fig. 6. When the equivalent stress distribution figure indicated the waves in the central strip is 5 IU, the equivalent stress distribution of the outermost strip of coil varied depending on the coiling tension. According to the analysis, we can see that when the value of local flatness and strip thickness were constant, the ridge-buckle value increased together with increasing coiling tension. For strip ridge buckles due to local waves, they can also be controlled by properly reducing coiling tension.

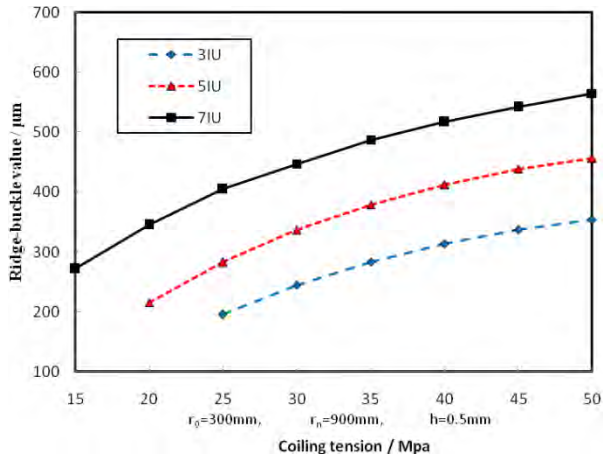

Figure 6: Relationship between coiling tension and ridge-buckle value.

4.3 Relationship between the size of the local waves and strip ridge-buckle value

Calculations were performed for ridge-buckle values of strip pieces with a coiling tension of 20-40 Mpa, an initial flatness value of 3-13 IU, strip strength of 0.5 mm and coil diameter respectively and the results are shown in Fig. 7. When the equivalent stress distribution figure indicated the coiling tension was 30 Mpa, the equivalent stress distribution of the outermost strip of coil varied depending on the local flatness value. It can be seen that when the strip thickness and coiling tension were constant, the ridge-buckle value increased along with increases of the initial flatness value. Therefore, the fundamental method to control coil ridge buckles is to decrease the local flatness defects of the strip in the coiling process.

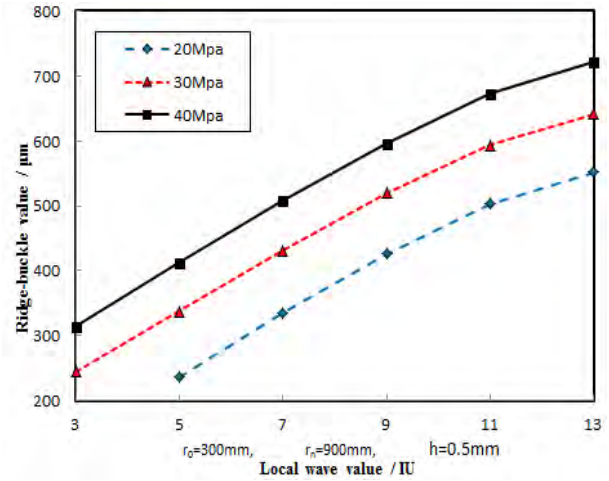

Figure 7: Relationship between local waves value and ridge-buckle value.

4.4 Relationship between the coil diameter and ridge-buckle value

Calculations were performed for ridge-buckle values of strip pieces with a coiling tension of 20-40 Mpa, thickness of 0.5 mm, coil diameter of 900 mm, local waves of 7 IU in the centre and different coil diameters respectively and the results are shown in Fig. 8. When the equivalent stress distribution figure indicated the coiling tension was 30 MPa, the equivalent stress distribution of the outermost strip of the coil varied depending on the coil diameter. According to the analysis, we can see that the ridge-buckle value increased along with increasing coil diameter. For a strip with local wave's defects, ridge buckles can also be controlled by properly dividing to reduce the coil diameter.

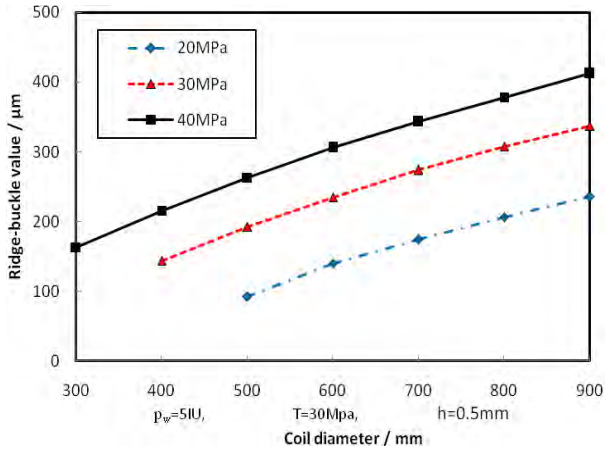

Figure 8: Relationship between coil diameter and ridge-buckle value.

4.5 Influence local waves location on ridge-buckle value

The influence of waves with different locations on strip ridge-buckle value was analysed to calculate ridge-buckle values of coils at the strip centre, 100 mm away from the centre, at a quarter of the strip width and at the strip edge with local waves of 9 IU, strip thickness of 0.5 mm and coil radius of 900 mm, respectively. The equivalent stress distribution figures show stress distribution of the coil at the strip centre, 100 mm away from the centre, at a quarter of the strip width and at the strip edge, and the calculation results are shown in Fig. 9.

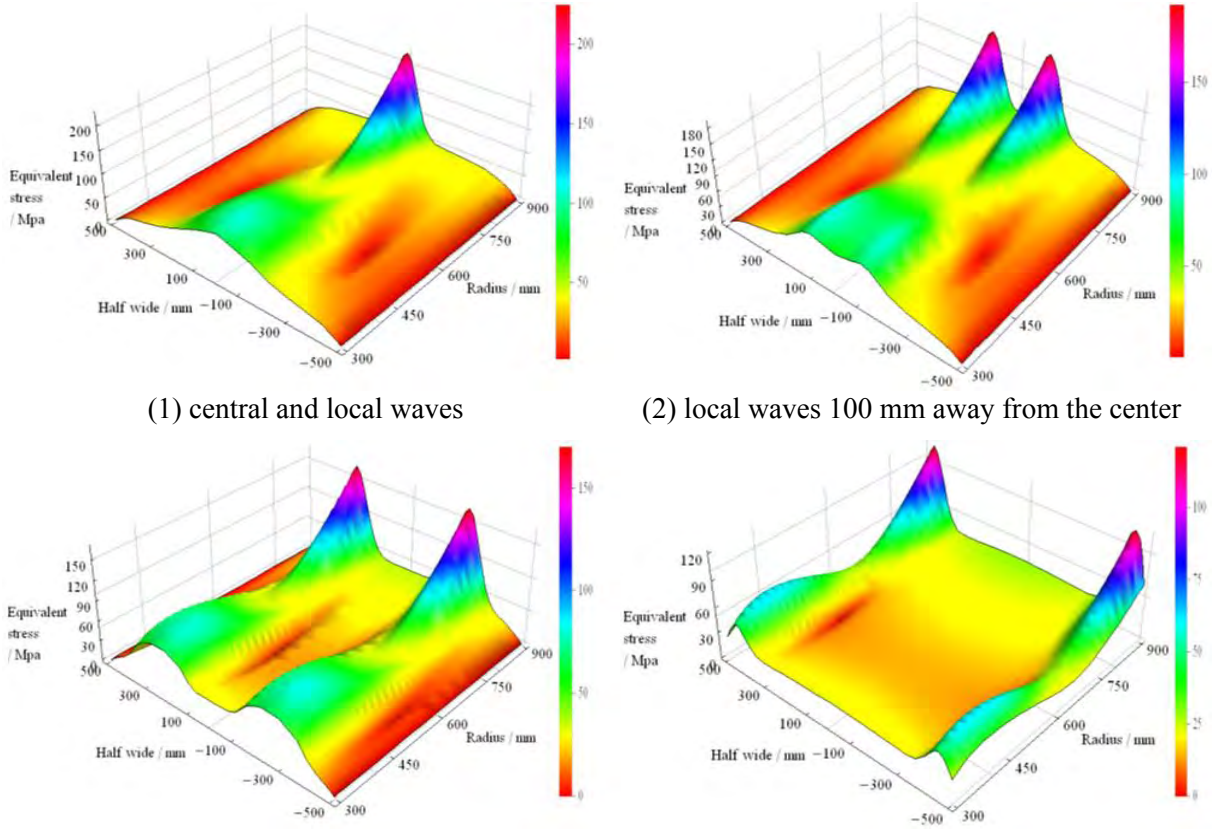

(1) central and local waves (2) local waves 100 mm away from the center

(3) local waves at a quarter (4) local waves at the edge

Figure 9: Stress distribution of the coil with different location of local waves.

From the equivalent stress figures of the coil with local waves with different location, the equivalent stress decreased from the strip centre to the edge along with waves location. When the waves lay at a quarter of the strip width or at the strip edge, the equivalent stress decreased sharply. Therefore, in the coiling process, ridge buckles are more likely to appear around the strip centre. Only with a larger local flatness value or coiling tension, will ridge buckles occur at the strip edge.

From Fig. 10 we can see that, when the coiling tension was the same, the strip ridge-buckle value decreased from the strip centre to edge along with local wave's location. Therefore, strip ridge buckles caused by local waves can be avoided by controlling the local wave's location using the rolling technique.

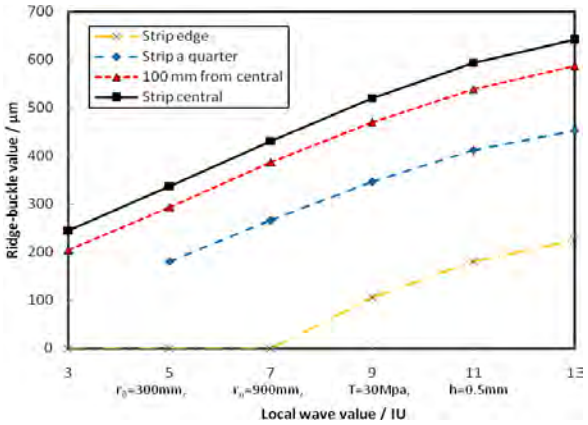

Figure 10: Influence of wave's location on ridge-buckle value.

5. VERIFICATION OF MODEL AND FE SIMULATION

In the actual production process, it is very difficult to accurately measure the stress distribution data of each layer in a coil. As a high precision tool for simulation use, commercial FE software enjoys high accuracy that has been verified by many practical cases [17, 18]. Therefore, for verification of algorithm accuracy of coiling tension and ridge-buckle model, it was performed in this paper by comparing with the calculation results obtained by general FE software ANSYS. In this paper, an ANSYS simulation model a steel coil was established by taking the parameters of Table 1 as an example, and the equivalent stress nephogram is shown in Fig. 11. On this basis, based on the mathematical simulation software Mathematic, an elastic ridge-buckle value calculation model program was set up to compare with the model presented in this paper.

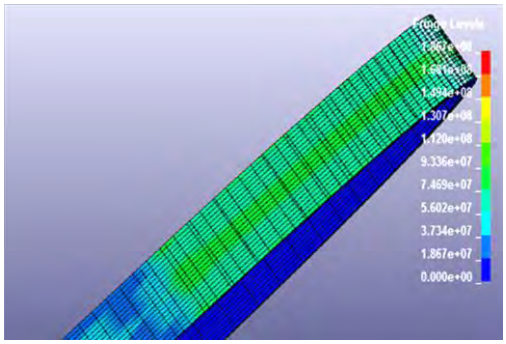

Figure 11: Equivalent stress of coiling strip.

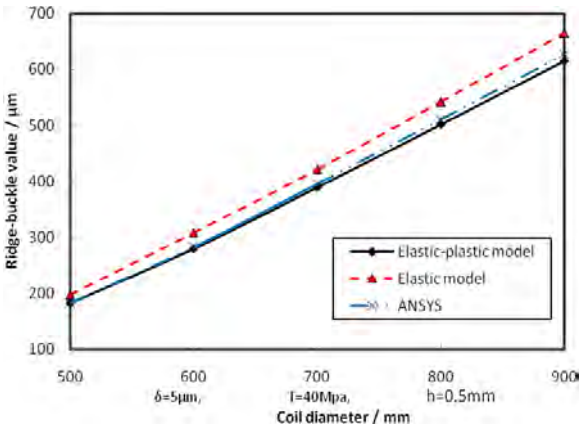

Figure 12: Comparison of ridge-buckle calculate model.

From Fig. 12, we can see that the equivalent stress distribution and ridge-buckle value obtained from the elastic-plastic model simulation were largely the same as the ANSYS FE simulation results, which verifies the accuracy and feasibility of this model. Due to the disregard of local plastic deformation of the strip and metal plastic flow by the elastic model, the precision of the result is bad and there is great difference between the calculated ridge-buckle values and the FE simulation results.

6. CONCLUSIONS

1) With reference to some ideas on how to deal with 3D elastic-plastic deformation and introduction of strip plastic flow factors, a coiling stress and ridge-buckle value model that can be used for online calculation was established; and the calculation accuracy and possibility of this model were verified by establishing a strip coiling FE simulation model and an elastic coiling stress and ridge-buckle value model to compare with the model presented in this paper.

2) With a quantitative analysis of the factors influencing the ridge-buckle value, the relevant rules that influence ridge buckles were obtained, which has laid a solid theoretical foundation for developing a coiling process system and handling on-site ridge-buckle defects in a scientific way with great practical value.

3) Secondary buckling as a result of sharply increased equivalent stress due to superposition of local waves was one of the main causes of more serious additional waves appearing if ridge buckles occur in a strip, and ridge buckles first appear on the outer coil layers; ridge-buckle value increased with increasing local waves, more obviously in thin strips than thick, and mostly appearing around in the strip centre and 100 mm away from the strip centre.

ACKNOWLEDGEMENT

This work was supported by Doctoral Program Foundation of Institutions of Higher Education of China (No. 20130006120024).

REFERENCES

[1] Bai, Z. H. (2009). *The core technology mathematical model for high-speed production of cold continuous rolling machine*, China Machine Press, Beijing, 28-32

[2] Melfo, W. M.; Dippenaar, R. J.; Carter, C. D. (2006). Ridge-buckle defect in thin-rolled steel strip, *Iron & Steel Technology*, Vol. 3, No. 8, 54-61

[3] Zhu, H. T.; Tieu, A. K.; Dippenaar, R. J.; Carter, C. D.; Ziegelaar, J. (2010). Effect of hot coil profile containing ridges on ridge-buckle defects of cold rolled thin strip, *International Journal of Material Forming*, Vol. 3, No. 1, 21-27, doi:10.1007/s12289-009-0412-1

[4] Melfo, W. M.; Dippenaar, R. J. (2005). Ridges in hot-rolled strip: Microstructural development as a function of temperature variations in the strip, *AISTech 2005 Conference Proceedings*, Vol. II, 295-306

[5] Melfo, W. M. (2006). Analysis of hot rolling events that lead to ridge-buckle defect in steel strips, PhD thesis, University of Wollongong, Wollongong

[6] Bai, Z. H.; Li, X. D. (2006). The influence that local waves shape brings to cold-rolled coiling strip ridge-buckle, *Mechanical Engineering Academic Journal*, Vol. 42, 229-232

[7] Ovesy, H. R.; Ghannadpour, S. A. M.; Zia-Dehkordi, E. (2013). Buckling analysis of moderately thick composite plates and plate structures using an exact finite strip, *Composite Structures*, Vol. 95, 697-704, doi:10.1016/j.compstruct.2012.08.009

[8] Lorenzini, G.; Helbig, D.; da Silva, C. C. C.; Real, M. V.; dos Santos, E. D.; Isoldi, L. A.; Rocha, L. A. O. (2016). Numerical evaluation of the effect of type and shape of perforations on the

buckling of thin steel plates by means of the constructal design method, *International Journal of Heat and Technology*, Vol. 34, Special Issue 1, S9-S20, doi:10.18280/ijht.34S102

[9] Ding, J. (2007). *Study on deformation of steel strip during coiling process*, University of Science and Technology Beijing, School of Mechanical Engineering, Beijing, 78-80

[10] Ghannadpour, S. A. M.; Ovesy, H. R.; Zia-Dehkordi, E. (2015). Buckling and post-buckling behaviour of moderately thick plates using an exact finite strip, *Computers and Structures*, Vol. 147, 172-180, doi:10.1016/j.compstruc.2014.09.013

[11] Sun, W. Q.; Li, B.; Shao, J.; He, A. R. (2016). Research on crown & flatness allocation strategy of hot rolling mills, *International Journal of Simulation Modelling*, Vol. 15, No. 2, 327-340, doi:10.2507/IJSIMM15(2)CO6

[12] Bush, A.; Nicholls, R.; Tunstal, J. (2001). Stress levels for elastic buckling of rolled strip and plate, *Ironmaking and Steelmaking*, Vol. 28, No. 6, 481-484, doi:10.1179/irs.2001.28.6.481

[13] Fischer, F. D.; Rammerstorfer, F. G.; Friedl, N. (2003). Residual stress-induced center wave buckling of rolled strip metal, *Journal of Applied Mechanics*, Vol. 70, No. 1, 84-90, doi:10.1115/1.1532322

[14] Liu, Y.-L.; Zhou, Y.; Fan, J.; Levick, M. (2011). Reduction of ridge buckles in cold rolled strip by using mill stands of different local rigidity, *Iron and Steel Technology*, Vol. 8, No 4, 250-259

[15] Jung, Y. J.; Lee, G. T.; Kang, C. G. (2002). Coupled thermal deformation analysis considering strip tension and with/without strip crown in coiling process of cold rolled strip, *Journal of Materials Processing Technology*, Vol. 130-131, 195-201, doi:10.1016/S0924-0136(02)00705-7

[16] Abdelkhalek, S.; Montmitonnet, P.; Legrand, N.; Buessler, P. (2011). Coupled approach for flatness prediction in cold rolling of thin strip, *International Journal of Mechanical Sciences*, Vol. 53, No. 9, 661-675, doi:10.1016/j.ijmecsci.2011.04.001

[17] Hatzenbichler, T.; Harrer, O.; Buchmayr, B.; Planitzer, F. (2010). Effect of different contact formulations used in commercial FEM software packages on the results of hot forging simulations, *La Metallurgia Italiana*, Vol. 7, No. 11-12, 11-15

[18] Annicchiarico, W. (2016). A structural shape optimization approach using flexible distributed evolution principles, *Revista de la Facultad de Ingeniería*, Vol. 31, No. 2, 46-65, doi:10.21311/002.31.2.02